SPIN CORRELATIONS IN HIGH Tc SUPERCONDUCTORS

Gen Shirane

JOURNAL DE PHYSIQUE
Colloque C8, Supplément au n° 12, Tome 49, décembre 1988

SPIN CORRELATIONS IN HIGH T_c SUPERCONDUCTORS

Gen Shirane

Brookhaven National Laboratory, Upton, New York 11973, U.S.A.

Abstract. – A review is given of current neutron scattering experiments on $La_{2-x}Sr_xCuO_4$ and $YBa_2Cu_3O_{6+x}$. Large single crystals have now been successfully grown for both of these high T_c superconductors and extensive measurements are being carried out on magnetic excitations for wide ranges of temperature and composition. A novel type of two-dimensional spin correlation is found with unusually large $J_{2D} \cong 1\,000$ K.

1. Introduction

The discovery [1] of superconductivity in doped-La_2CuO_4 and $YBa_2Cu_3O_{6-x}$ has stimulated extensive experimental and theoretical studies on these materials. Among many possible mechanisms, magnetism is now considered to play an essential role in superconductivity in these layer compounds [2]. We have carried out a series of neutron scattering measurements, in collaboration with scientists from many research institutes. Large single crystals are now available for La_2CuO_4, $La_{2-x}Sr_xCuO_4$ and $YBa_2Cu_3O_{6+x}$. This is a brief status report of on-going neutron scattering experiments in high T_c superconductors.

The first experimental confirmation of the antiferromagnetic long range order in La_2CuO_4 was reported by Vaknin *et al.* [3]. The magnetic structure is identical to that of the well-established two-dimensional (2D) antiferromagnet K_2NiF_4. The spin arrangement is shown in figure 1, and the insert demonstrates the special neutron scattering geometry used to secure the proper energy integration for the two-axis quasi-elastic scattering [4, 5]. The study of single crystal La_2CuO_4 revealed a novel magnetism of the 2D spin-$\frac{1}{2}$ antiferromagnet. This is depicted in figure 2; the integrated intensity across the sharp 2D ridge does not show a customary peak at T_N and fall off above. Instead it maintains high intensity as well as long correlation length ξ (> 200 Å) for a very wide temperature range. Another very important charasteristic of magnetism in La_2CuO_4 is the exceptionally large energy scale involved. this can be seen by a series of constant energy scans across the ridge: spin wave branches are so steep they can not be separated out up to $\Delta E = 12$ meV. The lower limit for the spin-wave velocity was estimated [2] at 0.4 eV Å and the recent high resolution experiment [6] revised this to 0.6 eV Å. Meanwhile, two magnon light scattering by Lyons *et al.* [7] also gave a high dispersion slope of 0.75 eV Å. Recent theoretical work by Chakravarty *et al.* [8] gave a consistent picture of these properties as unique characteristics of the spin-$\frac{1}{2}$ 2D antiferromagnet.

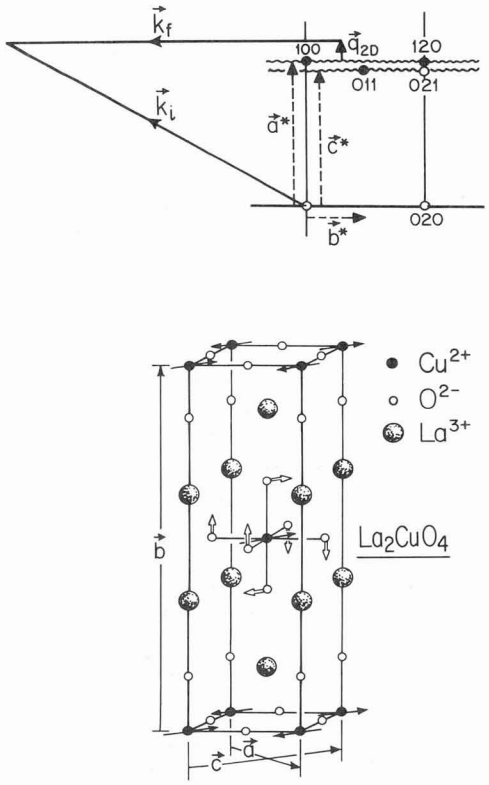

Fig. 1. – Magnetic structure of La_2CuO_4; the rotation of the CuO_6 octahedrons at the tetragonal-orthorhombic phase transition is illustrated. the upper part depicts the special scattering geometry for proper energy integration. After Endoh *et al.* [5].

It took somewhat longer to establish the magnetic ordering in $YBa_2Cu_3O_{6+x}$. Looking back, this was due to the unexpectedly high Néel temperature of 500 K in $O_{6.0}$. Assuming the Néel temperature must be below room temperature, early powder neutron scattering experiments failed to come up with different peaks between 300 K and 5 K. The muon spin rotation [9] gave the first experimental confirmation of magnetic order-

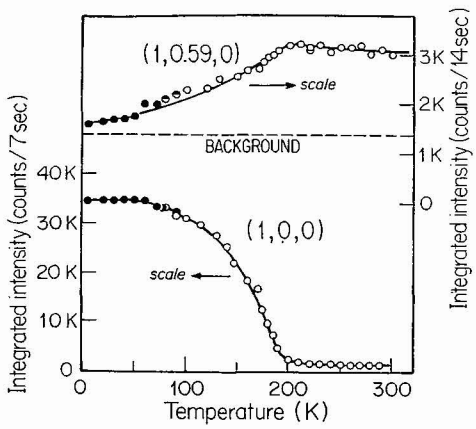

Fig. 2. – Integrated intensities of the (100) 3D antiferromagnetic Bragg peak and the (1, 0.59, 0) 2D ridge. After Shirane *et al.* [4].

ing at room temperature for $O_{6.0}$. Then the powder neutron scattering by Tranquada *et al.* [7] established the spin arrangement shown in figure 3. This magnetic structure, characterized by $\left(\frac{1}{2}\frac{1}{2}\ell\right)$ peaks with ℓ inte-

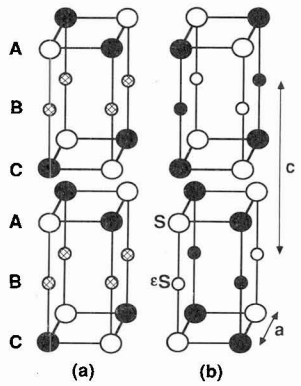

Fig. 3. – Magnetic structure for $YBa_2Cu_3O_{6+x}$ with x near zero. Cross-hatched circles represent non-magnetic Cu^{1+} ions, while filled and open circles indicate anti parallel spins at Cu^{2+} sites. After Tranquada *et al.* [10].

ger, reveals an interesting distribution of Cu moments in this crystal. Solid and open circles represent ± spins of Cu^{2+} in A and C CuO_2 layers. Cross hatched circles represent, in O_6 composition, non-magnetic Cu^{1+} ions. Later we will demonstrate that a different magnetic structure appears when this magnetically dead layer is activated at higher oxygen concentration. The phase diagram was determined by muon [9] and neutron scattering [10] and is shown in figure 4. There is a sharp drop of the Néel temperature around $O_{6.4}$ and the nature of magnetism at higher oxygen concentration (superconducting) is not yet understood.

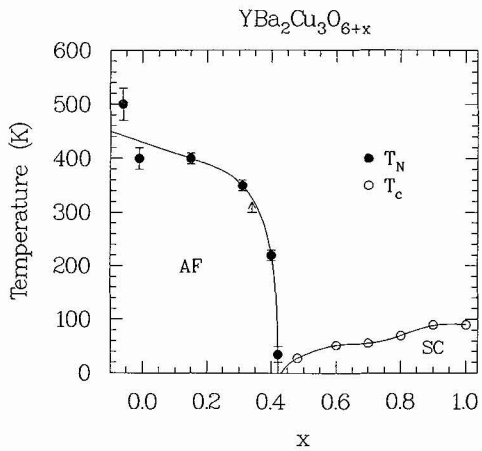

Fig. 4. – Phase diagram for $YBa_2Cu_3O_{6-x}$ showing Néel temperatures determined by neutron diffraction. After Tranquada *et al.* [10].

2. $La_{2-x}Sr_xCuO_4$

We have just surveyed the magnetic phase diagram of $YBa_2Cu_3O_{6-x}$ where an antiferromagnetic phase is observed over a wide range of oxygen content. In contrast, the antiferromagnetic Néel temperature in La_2CuO_4 is very sensitive to doping and is rapidly lowered by a slight increase of oxygen content [3, 11] or even 1 % doping of Sr. Since Sr doping creates superconductivity [1] around $x = 0.05 - 0.20$, it is of great interest to study how magnetic correlations are changed by doping; This requires a series of large crystals of known Sr concentrations. Extensive neutron scattering experiments were carried out at Brookhaven on crystals grown at MIT, NTT and IMS and results were reported very recently by Birgeneau *et al.* [6].

Figure 5 shows variouss properties of $La_{2-x}Sr_xCuO_4$ crystals as a function of Sr concentration x. The overall tendencies are well established even though data fluctuations are large. The top figure shows the concentration dependence of the orthorhombic-tetragonal phase transition T_{ST}, which is in agreement with the previous powder data [12]. These doped crystals usually contain some impurity phases and are not as clean as pure La_2CuO_4. Nevertheless reasonably good two-axis quasielastic scattering data are obtained as shown in figure 6. These experiments utilize the special scattering geometry depicted in figure 1 so that the proper energy integration is achieved. Figure 7 summarized the overall results for the correlation length ξ as a function of x up to 0.18. The solid line represents a simple model calculation of the average distance between holes when the doping creates holes in O^{2-} randomly. The observed ξ approximately follow the line. One very important result not shown in these figures

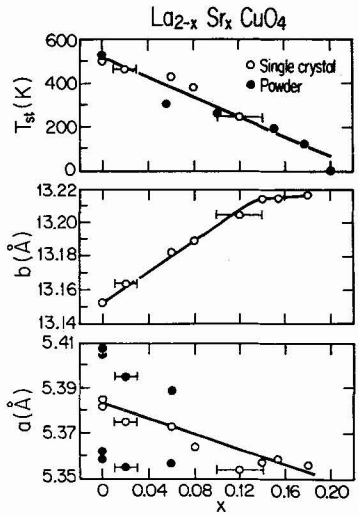

Fig. 5. – Room temperature lattice constants and structural phase transition temperatures in single crystal and powder samples of $La_{2-x}Sr_xCuO_4$. After Birgeneau *et al.* [6].

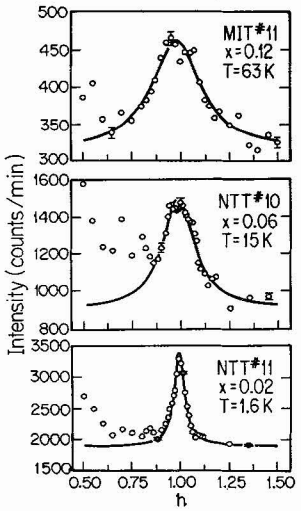

Fig. 6. – Examples of two axis scans across the ridge along (1, ζ, 0) in $La_{2-x}Sr_xCuO_4$. After Birgeneau *et al.* [6].

is the x dependence of the average magnetic moment. The size of each crystal is normalized by the intensity of standard phonons so that magnetic scattering of all Sr-doped samples can be compared to each other. The normalized magnetic intensities are essentially independent of Sr concentratiolns even into the superconducting range. Thus the doping does not change the magnetic moment but is shortens the correlation length. No important differences in the magnetic scattering are observed in the normal and superconducting statesw. So far neutron scattering expriments were

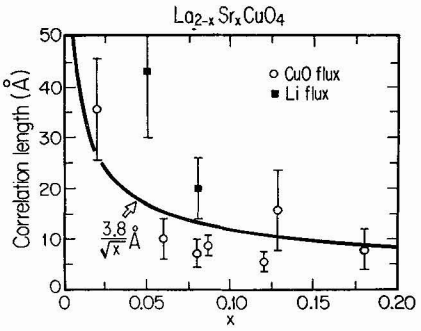

Fig. 7. – Antiferromagnetic correlation length *versus* concentration in $La_{2-x}Sr_xCuO_4$. The solid line is the function $3.8/\sqrt{x}$ Å which is the average separation between the holes introduced by the Sr doping. After Birgeneau *et al.* [6].

carried out on Sr-doped crystals with a Meissner fraction less than 20 % . The next step is to carry out magnetic scattering experiments on doped crystals with a very high Meissner fraction.

3. $YBa_2Cu_3O_{6+x}$

The basis antiferromagnetic structure and the magnetic phase diagram for this family of high T_c compounds were already shown in figures 3 and 4. All powder samples studied so far [10, 13] show the same type of magnetic structure characterized by $\left(\frac{1}{2}\frac{1}{2}\ell\right)$ with ℓ integer. However, a single crystal studied by Kadowaki *et al.* [14] revealed a new spin arrangement at low temperature. This antiferromagnetic arrangement is shown in figure 8b and characterized by $\left(\frac{1}{2}\frac{1}{2}\ell\right)$ with

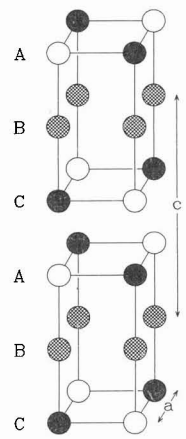

Fig. 8. – The second magnetic structure (b) for $YBa_2Cu_3O_{6+x}$, which gives $\left(\frac{1}{2}\frac{1}{2}\ell\right)$ with ℓ half integer. Small circles are ordered moments in oxygen deficient planes. After Kadowaki *et al.* [14]. Figure a is the same as figure 3.

ℓ half integer. This second type of magnetic structure was also observed in $NdBa_2Cu_3O_{6+x}$ crystals [15]. The temperature dependence of magnetic intensities in an $YBa_2Cu_3O_{6.35}$ single crystal [14] is shown in figure 9.

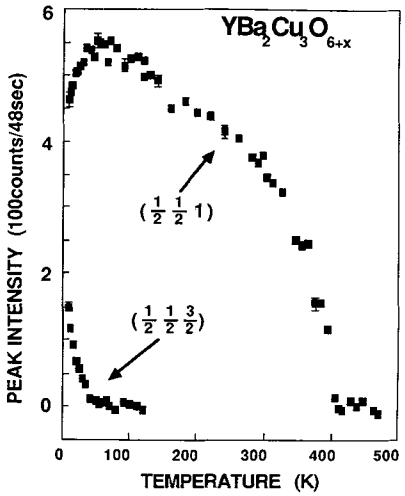

Fig. 9. – Peak intensities of $\left(\frac{1}{2}\frac{1}{2}1\right)$ and $\left(\frac{1}{2}\frac{1}{2}\frac{3}{2}\right)$ magnetic reflections as a function of temperature for a single crystal of $YBa_2Cu_3O_{6.35}$. After Kadowaki *et al.* [14].

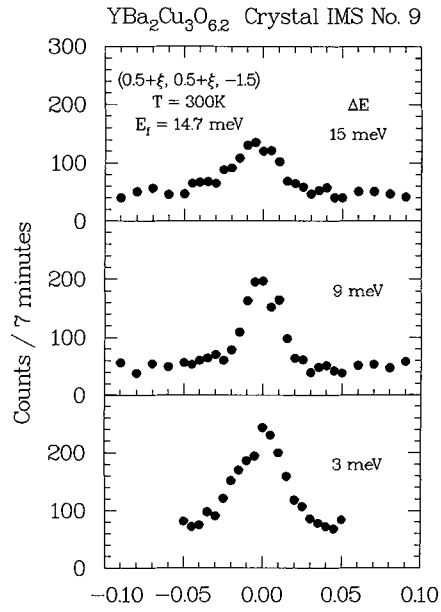

Fig. 10. – Constant E scans for a large single crystal of $YBa_2Cu_3O_{6.2}$. After Sato *et al.* [17].

As the intensity of the $\left(\frac{1}{2}\frac{1}{2}1\right)$ peak decreases below 50 K, the $\left(\frac{1}{2}\frac{1}{2}\frac{3}{2}\right)$ peak comes up. This new structure is actually the natural spin arrangement for compositions O_{6-x} where Cu^{2+} spins are introduced into the chain layers. Then the spin configuration in figure 3 is unstable because A and C must have the same spin direction, irrespective of the sign of the AB (and BC) interaction. At present, a simple magnetic phase diagram for the two spin structures is not yet established. This is a probably due to insufficient control of the true chemical compositions of $YBa_2Cu_3O_{6-x}$. Further study is needed to fully understand this point.

Until very recently, a large enough crystal of $YBa_2Cu_3O_{6+x}$ was not available for inelastic neutron scattering studies. Shamoto, Hosyoya and Sato [16] were the first to accomplish this difficult task of growing a large O_{6+x} magnetic crystal. The neutron scattering experiment followed immediately [17], with the results shown in figure 10. Just as in La_2CuO_4, a very steep magnon dispersion was observed for an $O_{6.2}$ single crystal with $T_N = 100$ °C. The slope of the dispersion is so steep that it is not possible to resolve the peak into two separate branches. However, one can place the lower limit of the slope at 0.5 eV Å; this is in good agreement with the result of two-magnon Raman scattering by Lyons *et al.* [18]. Further details of this study will be reported shortly.

There is one very important question that remains in $YBa_2Cu_3O_{6+x}$. This concerns the nature of the magnetic interactions in $O_{6.4}$ and higher oxygen compositions where superconductivity sets in and reaches 95 K at $O_{7.0}$. Lyons *et al.* [18] reported that the magnetic coupling persists into $O_{6.6}$ and $O_{6.9}$, although the Raman peak broadens and shifts to lower frequencies. Can the antiferromagnetic correlation in O_7 be directly observed by the neutron scattering technique, as was the case in $La_{1.85}Sr_{0.15}CuO_4$? We hope to answer this question in the near future.

Acknowledgments

This brief review summarized a series of exciting neutron scattering experiments at Brookhaven in collaboration with many scientists, in particular R. J. Birgeneau, Y. Endoh, Y. Hidaka, M. Sato, S. K. Sinha, and J. M. Tranquada. I have also benefited by many stimulating discussions with J. D. Axe, V. J. Emery, M. Strongin, and Y. J. Uemura. This work was supported by the U.S. Japan Cooperative Neutron Scattering Program and research at Brookhaven is supported by the Division of Materials Sciences, U.S. Department of Energy under contract DE-AC02-76CH00016.

[1] Bednorz, J. G. and Müller, K. A., *Z. Phys. B* **64** (1986) 189;
Wu, M. K. *et al., Phys. Rev. Lett.* **58** (1987) 908.
[2] For example see: Anderson, P. W., *Science* **235** (1987) 1196;
Emery, V. J., *Phys. Rev. Lett.* **58** (1987) 2794;
Hirsch, J. E., ibid., **59** (1987) 228;
Schrieffer, J. R. *et al.,* ibid., **60** (1988) 944;
Aharony, A., *et al.,* ibid., **60** (1988) 1330.
[3] Vaknin, D; *et al., Phys. Rev. Lett.* **58** (1987) 2802.
[4] Shirane, G. *et al., Phys. Rev. Lett.* **59** (1987) 1613.
[5] Endoh, Y. *et al., Phys. Rev. B* **37** (1988) 7443.
[6] Birgeneau, R. J. *et al., Phys. Rev. B* **38** (1988) 6614.
[7] Lyons, K. B. *et al., Phys. Rev. B* **37** (1988) 2393.
[8] Chaakravarty, S., Halperin, B. I. and Nelson, D. R., *Phys. Rev. Lett.* **60** (1988) 1057.
[9] Nishida, N. *et al., Jpn J. Appl. Phys.* **26** (1987) L 1856,
Brewer, J. H., *Phys. Rev. Lett.* **60** (1988) 1073.
[10] Tranquada, J. M., *et al., Phys. Lett.* **60** (1988) 156;
Tranquada, J. M. *et al., Phys. Rev. B* **38** (1988) 2477.
[11] Freltoft, T. *et al., Phys. Rev. B* **36** (1987) 826;
Yamada, K. *et al., Solid State Commun.* **64** (1987) 753.
[12] Fleming, R. M., Batlogg, B., Cava, R. J. and Kietman, E. A., *B* **35** (1987) 7191.
[13] Li, W. H. *et al., Phys. Rev. B* **37** (1988) 9844.
[14] Kadowaki, H. *et al., Phys. Rev. B* **37** (1988) 7932.
[15] Moudden, H. *et al., Phys. Rev. B* **38** (Nov. 1988).
Lynn, J. W. *et al., Phys. Rev. Lett.* **60** (1988) 2781.
[16] Shamoto, S., Hosoya, S. and Sato, M., *Solid State Commun.* **66** (1988) 95.
[17] Sato, M., Shamoto, S., Tranquada, J. M. and Shirane, G., *Phys. Rev. Lett.* **61** (1988) 1317.
[18] Lyons, K. B. *et al., Phys. Rev. Lett.* **60** (1988) 732.